INTERNATIONAL JOURNAL OF MATHEMATICS AND COMPUTER RESEARCH

Using an Oblique Projection Operator for DOA Estimation Of Uniform Linear Array In The Presence Of Mutual Coupling

[1]Chien-Chou Lin,[2]Ya-Ling Chen

[1]General Education Center, National Taipei University of Technology, 1 Sec. 3, Zhongxiao E. Rd.
Taipei 10608, Taiwan
[2]Department of Accounting Information, National Taichung University of Science and Technology,
129 Sec 3, Sanmin Rd. Taichung 40401, Taiwan
[1]E-mail: linjj@ntut.edu.tw
[2]E-mail: ylcheng@nutc.edu.tw.

Abstract

Oblique projection operator (OPO)can be used to project measurements onto a low-rank desired signal subspace along a direction thatis oblique to the subspace. The appropriate subspace projection may be used to enhance the characteristics of the desired signal power and reduces the interference effect. In this paper,we propose a high-resolution direction-of-arrival(DOA)estimation algorithm for signal sources of uniform linear array (ULA) in the presence of mutual coupling by using an oblique projection operator. The mutual coupling coefficient between two sensor elements is inversely proportional to their distance and the value can be approximated as zero when the distance is far enough. The mutual coupling matrix (MCM) of a ULA can be expressed as a banded symmetric Toeplitz matrix. The multiple signal classification (MUSIC)algorithm by using an orthogonal projection operator for DOA estimation in the presence of mutual coupling signal environments can only utilize the middle subarray, the DOA estimation is biased. We usean oblique projection operator on a beam space to overcome the drawback of MUSIC algorithm for DOA estimation in the presence of mutual coupling and the algorithm proceeds into two stages. First, we use MUSIC algorithm to obtain the estimated DOAs of the signal sources. Because the estimation sareprone to bias, we built a beam space near the estimated angles in Stage 1 to reduce DOA bias. Next, the projection weights of steering vectors on signal subspaces were replaced with their revised steering vectors. We use an oblique projection operator on the beam space to develop the characteristic of DOA of signal sources on a spatial spectrum for scanning and estimating the angle-of-arrival of signal sources. High-resolution DOA estimates are thus obtained. Finally, simulation results demonstrate the performance and procedural accuracy of our method.

Keywords: Direction-of-arrival (DOA), multiple signal classification (MUSIC), oblique projection operator, beam space, mutual coupling

Introduction

The projection operators can be into orthogonal and oblique operators. Orthogonal projection operators arise naturally in the optimal solutions of many problems in DOA estimation [3–4].Oblique projection operator (OPO) can be used to project measurements onto a low-rank desired signal subspace along a direction that is oblique to the subspace. The appropriate subspace projection can be used to enhance the characteristics of the desired signal power and reduces the interference effect. In the recent years, oblique projection operators has received a lot of attention in signal processing[15-18].

The direction-of-arrivals (DOAs) estimation of signals impinging on an array of sensors is the fundamentals of employing array processing in various applications related to radar, sonar, communications, and astronomy. A number of subspace high-resolution DOA estimation has been developed, including the multiple signal classification (MUSIC) and the estimation signal parameter via a rotational invariant technique (ESPRIT) [3–4].These conventional high-resolution DOA estimation methods generally need a prior knowledge of array manifold. Their performance will be distorted by the unknown array manifold errors, such as the mutual coupling of the interaction between the sensor elements. The DOA estimation in the presence of unknown mutual coupling attracts an extensive attention, many mutual coupling calibration

methods has been proposed [6-14]. Making use of the calibration sources with known locations, a maximum-likelihood calibration method proposed in [7] can compensate the mutual coupling as well as gain, phase and sensor position errors. In real system it may be difficult to obtain calibration sources, the methods in [8-11] is another kind of array calibration methods which do not require the calibration sources at known location, called auto-calibration. Auto-calibration is more preferable method, since it can be estimate the DOAs and the mutual coupling coefficients simultaneously. The mutual coupling auto-calibration method proposed by Friedlander et al [8] and Selloneet al [9] present an iterative procedure to estimate the DOA sand mutual coupling coefficients. However, there are a great number of unknown parameters involved in these two methods lead their computation is high and complexities. So it may not be to suitfor real-time applications and may alsonot be convergent [11-14].

In orderto overcome the shortcomings of mutual coupling auto-calibration methods presented above.In [13-14], mutual coupling calibration methods for ULA are proposed. These methods are based on the fact that the mutual coupling coefficient between two sensor elements is inversely proportional to their distance and the value can be approximated as zero when the distance is far enough. The mutual coupling matrix (MCM) of a ULA can be expressed as a banded symmetric Toeplitz matrix, and then the number of unknown parameters isreduced significantly. In [13], the DOAs of uncorrelated signals estimated by a reduced array with unknown mutual coupling. Unlike the MUSIC algorithm directly for DOA estimation, only the middle subarray is utilizedin the presence of mutual coupling, in [14] propose a method which use the whole array, instead of the middle subarray,to improve the accuracy of DOA estimation.

The oblique projection operator (OPO) was introduced to estimate DOA of signal sources in [15-18]. An OPO which is established by projecting the desired source signal subspaceuse to extract the desired source signal covariance from the source signal covariance matrix. The numerical simulation shows that the estimation of DOAs for high correlated or coherent signal sources performance well.

In this paper, we propose a high-resolution DOA estimation method for the incident DOA ofuncorrelated signal sources in the presence of mutual coupling. This method proceeds into two procedures. First, we useMUSIC algorithm to obtain DOA estimates for one set of signal sources, which is expected to show a bias in the estimation, and we rebuilt a new steering matrix near the estimated DOAs angle. The original collected data are projected on the beam space extended from the steering vectors to build a new set of data [19-22].Next, OPO [15-18] on the beam space is employed to develop the characteristic of DOAs of signal sources on a spatial spectrum for scanning and estimating the angle-of-arrival of the signal sources.

This rest of this paper is organized as follows. A simple description of the data model is introduced in Section 2. The beam space, the OPO built on the beam space, and our algorithm are introduced in Section 3.The computer simulation results for showing our algorithm's estimation performance are presented in Section 4.We conclude this paper in Section 5.

Data Model

Assume that a D number of far-field narrow band uncorrelated signal sources enter a uniform linear array made up of M sensors at varying angles-of-arrival $\{\theta_1, \theta_2, \cdots, \theta_D\}$, that the spacing constant between the two adjacent antenna component sis$d$, where $d$is $\frac{1}{2}$ of the wavelength. Let $\mathbf{a}(\theta_i) = [a_1(\theta_i), a_2(\theta_i), \cdots, a_M(\theta_i)]^T$ be the steering vector of the angle-of-arrival θ_i in the $M \times 1$ dimension, then $a_k(\theta) = \exp[-j2\pi d(k-1)\sin\theta/\beta]$ is the response of the incident signal coming from the kth sensor from the angle-of-arrival θ at unit amplitude $j = \sqrt{-1}$, and β is the wavelength of the signal carrier. In the presence of the mutual coupling environment, the data vector of the array sensors at time t and $M \times 1$ dimension canthus be written as:

$$\mathbf{x}(t) = \sum_{i=1}^{D} \mathbf{C}\mathbf{a}(\theta_i)s_i(t) + \mathbf{n}(t) = \mathbf{A}\mathbf{s}(t) + \mathbf{n}(t) \tag{1}$$

where $t = 1, 2, \cdots, N$ and N is the number of snapshots.In particular, $\mathbf{C}$ is the $M \times M$ dimension mutual coupling matrix (MCM) of a ULA$\mathbf{s}(t) = [s_1(t), s_2(t), \cdots, s_D(t)]^T$ isthe $D \times 1$ dimension vectors composed of

signal amplitudes, $\mathbf{A} = [\mathbf{a}(\theta_1), \mathbf{a}(\theta_2), \cdots, \mathbf{a}(\theta_D)]$ represents the steering matrix in the $M \times D$ dimension, where the superscript Trepresents transposition. The noise $\mathbf{n}(t)$ of the array sensors is the zero-mean spatially white Gaussian process not correlated with any of the signal sources. The noise covariance matrix is thus the following unknown diagonal matrix.

$$\mathbf{R}_n = E\{\mathbf{n}(t)\mathbf{n}^H(t)\} = \sigma_n^2 \cdot \mathbf{I}_M \tag{2}$$

where $E\{\square\}$ and the superscript H represent the expected value and the complex conjugate transpose, respectively, and $\mathbf{I}_M$ is the unit matrix in the $M \times M$ dimension.

In practice, the mutual coupling coefficient coefficients between two sensor elements is inversely proportional to their distance and the value can be approximated as zero when the distance is far enough. The mutual coupling matrix (MCM) $\mathbf{C}$ of a ULA can be expressed as a banded symmetric Toeplitz matrix [8-14]. More precisely, the mutual coupling coefficient can be approximated to be zero when the distance between two sensor elements is more than p inter-sensor spacing. Here, we assume there are only $p+1$ nonzero mutual coupling coefficients. As a result, $\mathbf{C}$ can be expressed as a band symmetric Toeplitz matrix as follows [8-14]

$$\mathbf{C} = \begin{bmatrix} 1 & c_1 & \cdots & c_p & & & & \\ c_1 & 1 & c_1 & \cdots & c_p & & 0 & \\ \vdots & \ddots & \ddots & \ddots & \vdots & \ddots & & \\ c_p & \cdots & c_1 & 1 & c_1 & \cdots & c_p & \\ & \ddots & \vdots & \ddots & \ddots & \ddots & \vdots & \ddots \\ & & c_p & \cdots & c_1 & 1 & c_1 & \cdots & c_p \\ & & & \ddots & \vdots & \ddots & \ddots & \ddots & \vdots \\ & 0 & & & c_p & \vdots & c_1 & 1 & c_1 \\ & & & & & c_p & \cdots & c_1 & 1 \end{bmatrix}_{M \times M} . \tag{3}$$

In the presence of mutual coupling, the realsteering vector should be re written as $\mathbf{a}_c(\theta_i) = \mathbf{C}\mathbf{a}(\theta_i)$, for $i = 1, 2, \cdots, D$. For simplicity of notation, we denote $\mathbf{A}_c = \mathbf{C}\mathbf{A}$, then

$\mathbf{A}_c = \mathbf{C}\mathbf{A} = [\mathbf{C}\mathbf{a}(\theta_1), \mathbf{C}\mathbf{a}(\theta_2), \cdots, \mathbf{C}\mathbf{a}(\theta_D)] = [\mathbf{a}_c(\theta_1), \mathbf{a}_c(\theta_2), \cdots, \mathbf{a}_c(\theta_D)]$. Thus the $M \times 1$ array output vector can then be represented by the following model

$$\mathbf{x}(t) = \mathbf{A}_c \mathbf{s}(t) + \mathbf{n}(t). \tag{4}$$

The source signal covariance matrix is

$$\mathbf{R}_s = \mathbf{A}_c(\theta)E\{\mathbf{s}(t)\mathbf{s}^H(t)\}\mathbf{A}_c^H(\theta) = \mathbf{A}_c(\theta)\mathbf{S}\mathbf{A}_c^H(\theta) \tag{5}$$

where

$$\mathbf{S} = E\{\mathbf{s}(t)\mathbf{s}^H(t)\} \tag{6}$$

The array output vector of array sensors in the $M \times M$ dimension has the following covariance matrix:

$$\begin{aligned} \mathbf{R}_x &= E\{\mathbf{x}(t)\mathbf{x}^H(t)\} \\ &= \mathbf{A}_c E\{\mathbf{s}(t)\mathbf{s}^H(t)\}\mathbf{A}_c^H + E\{\mathbf{n}(t)\mathbf{n}^H(t)\} \\ &= \mathbf{A}_c \mathbf{S} \mathbf{A}_c^H + \sigma_n^2 \cdot \mathbf{I}_M \\ &= \mathbf{R}_s + \mathbf{R}_n. \end{aligned} \tag{7}$$

Here, the covariance matrix of array output vector of array sensors $\mathbf{R}_x$ can be substituted by the received limited sample mean $\hat{\mathbf{R}}_x = (1/N)\sum_{k=1}^{N} \mathbf{x}(k)\mathbf{x}^H(k)$, where N is the number of snapshots.

The eigen value decomposition (EVD) of $\mathbf{R}_x$ can beproducing the following equation:

$$\mathbf{R}_x = \sum_{m=1}^{D} \lambda_m \mathbf{e}_m \mathbf{e}_m^H + \sum_{m=D+1}^{M} \lambda_m \mathbf{e}_m \mathbf{e}_m^H = \mathbf{E}_s \mathbf{\Lambda}_s \mathbf{E}_s^H + \mathbf{E}_n \mathbf{\Lambda}_n \mathbf{E}_n^H \tag{8}$$

where $\lambda_1 \geq \lambda_2 \geq \cdots \geq \lambda_D \geq \lambda_{D+1} = \cdots = \lambda_M = \sigma_n^2$ and is the eigen value of $\mathbf{R}_x$; the $\mathbf{e}_m$ is the eigenvector of unit norm corresponding to λ_m, for $m = 1, 2, \cdots, M$, respectively. Each vector of $\mathbf{E}_s = [\mathbf{e}_1, \mathbf{e}_2, \cdots, \mathbf{e}_D]$ is perpendicular to that of $\mathbf{E}_n = [\mathbf{e}_{D+1}, \cdots, \mathbf{e}_M]$, and $\mathbf{\Lambda}_n = \sigma_n^2 \mathbf{I}_{M-D}$ is the eigen value diagonal matrix of $\mathbf{R}_n$. When the D signal sources are not correlated and $M > D$, then $E\{s_i(t)s_i^H(t)\}$, for $i = 1, 2, \cdots, D$ is the power of each source signal; when $E\{s_i(t)s_j^H(t)\} = 0$, for $i \neq j$, then the rank of $\mathbf{R}_s$ is D.

The signal subspace and noise subspace is spanned by $\mathbf{E}_s$ and $\mathbf{E}_n$, respectively, From the principle of subspace, $\mathbf{E}_s$ and the signal steering vector matrix $\mathbf{A}_c$ demonstrate an identical signal subspace and $\mathbf{E}_s \perp \mathbf{E}_n$ [3]. The vertical projection operator (VPO) $\mathbf{P}_{\mathbf{E}_s}$ in the signal subspace and noise subspace are perpendicular to each other ($\mathbf{P}_{\mathbf{E}_s} \perp \mathbf{P}_{\mathbf{E}_n}$). Because the signal subspace and noise subspace are orthogonal, the MUSIC algorithm [3] with MCM can be implemented to estimates the DOAs of the signal sources in the presence of mutual coupling from the MUSIC spatial spectrum as

$$J_{\mathrm{MUSIC}}(\theta) = \max_\theta \frac{1}{\left|\mathbf{a}_c^H(\theta)\mathbf{P}_{\mathbf{E}_n}\mathbf{a}_c(\theta)\right|} = \max_\theta \frac{1}{\left|\mathbf{a}_c^H(\theta)\mathbf{E}_n\mathbf{E}_n^H\mathbf{a}_c(\theta)\right|} \qquad (9)$$

In the presence of mutual coupling environment, the MUSIC algorithm produce biased DOA estimates. To reduce the estimation biases, we use the OPO [15-18] on the beam space to build the characteristics of the source signal DOAs on the spatial spectrum for scanning and estimating the angle-of-arrival of a source signal to obtain high-resolution estimations. We thus propose the following algorithm.

Proposed Algorithm
In this paper, we proposed a high-resolution method for estimating DOAs of signal sources in the presence of mutual coupling. The method was divided into two stages: first, the DOA estimates of a group of signal sources were obtained using (9) and the signal sources directions were determined. Second, we rebuilt a new steering matrix near the estimated DOA angle found in Stage One. In addition, the original collected data were projected on the beam space extended from steering vectors to build a new set of data and OPO, which were used to separate the desired source signal from the source signal subspace. The desired source signal covariance to be estimated was extracted from the source signal covariance matrix to build the characteristics of the source signal DOAs on the spatial spectrum. Stages 1 and 2 are described as follows.

Stage 1: (9) was used to obtain DOA estimates for the signal sources $\{\theta_1, \theta_2, \cdots, \theta_D\}$. Next, by referring to [18, 21–22], $\frac{1}{2}$ was chosen as the resolution of the left and ride side of θ_i to obtain θ_{i^-} and θ_{i^+}.

Stage 2: A $M \times 3D$ dimensional matrix was adopted. $\mathbf{W} = [\mathbf{a}(\theta_{1^-}), \mathbf{a}(\theta_1), \mathbf{a}(\theta_{1^+}), \mathbf{a}(\theta_{2^-}), \mathbf{a}(\theta_2), \mathbf{a}(\theta_{2^+}), \cdots, \mathbf{a}(\theta_{D^+})]$ we rebuilt a new steering matrix. Subsequently, the original collected data were projected on the beam space extended from the steering vectors to build a new set of data. The new data output was written as a $3D \times 1$ dimensional vector $\mathbf{y}(t) = \mathbf{W}^H \mathbf{x}(t)$, where

$$\begin{aligned} \mathbf{y}(t) &= \mathbf{W}^H \mathbf{x}(t) \\ &= \mathbf{W}^H \mathbf{A}_c \mathbf{s}(t) + \mathbf{W}^H \mathbf{n}(t). \end{aligned} \qquad (10)$$

$$\text{Let } \overline{\mathbf{A}} = \mathbf{W}^H \mathbf{A}_c \text{ and } \overline{\mathbf{n}}(t) = \mathbf{W}^H \mathbf{n}(t),$$

$$\begin{aligned} \overline{\mathbf{A}} &= \mathbf{W}^H \mathbf{A}_c \\ &= \left[\mathbf{W}^H \mathbf{a}_c(\theta_1), \mathbf{W}^H \mathbf{a}_c(\theta_2), \cdots, \mathbf{W}^H \mathbf{a}_c(\theta_D) \right] \\ &= [\overline{\mathbf{a}}(\theta_1), \overline{\mathbf{a}}(\theta_2), \cdots, \overline{\mathbf{a}}(\theta_D)]. \end{aligned} \qquad (11)$$

$\overline{\mathbf{A}}$ in beam space processing served the same role as $\mathbf{A}_c$ in element-space processing. Therefore,

$$\mathbf{y}(t) = \overline{\mathbf{A}}\mathbf{s}(t) + \overline{\mathbf{n}}(t). \qquad (12)$$

From (10), the $\mathbf{y}(t)$ covariance matrix was written as

$$\overline{\mathbf{R}}_y = E\{\mathbf{y}(t)\mathbf{y}^H(t)\} = \overline{\mathbf{A}}\mathbf{S}\overline{\mathbf{A}}^H + E\{\overline{\mathbf{n}}(t)\overline{\mathbf{n}}^H(t)\}. \tag{13}$$

Let $\overline{\mathbf{R}}_s = \overline{\mathbf{A}}\mathbf{S}\overline{\mathbf{A}}^H$ and $\overline{\mathbf{R}}_n = E\{\overline{\mathbf{n}}(t)\overline{\mathbf{n}}^H(t)\}$, then(13) could be re-written as

$$\overline{\mathbf{R}}_y = \overline{\mathbf{R}}_s + \overline{\mathbf{R}}_n. \tag{14}$$

$\overline{\mathbf{R}}_y$ underwent eigen value decomposition [19–20], which could be represented as

$$\begin{aligned}
\overline{\mathbf{R}}_y &= E\{\mathbf{y}(t)\mathbf{y}^H(t)\} \\
&= \sum_{m=1}^{D} \gamma_m \mathbf{v}_m \mathbf{v}_m^H + \sum_{m=D+1}^{3D} \gamma_m \mathbf{v}_m \mathbf{v}_m^H \\
&= \overline{\mathbf{E}}_s \overline{\mathbf{\Lambda}}_s \overline{\mathbf{E}}_s^H + \overline{\mathbf{E}}_n \overline{\mathbf{\Lambda}}_n \overline{\mathbf{E}}_n^H.
\end{aligned} \tag{15}$$

where $\gamma_1 \geq \gamma_2 \geq \cdots \geq \gamma_D \geq \gamma_{D+1} = \cdots = \gamma_{3D} = \sigma_n^2$ and was the eigenvalue of $\overline{\mathbf{R}}_y$ and corresponds to the eigenvector $\mathbf{v}_m$ of γ_m, for $m = 1, 2, \cdots, 3D$. $\langle \overline{\mathbf{E}}_s \rangle$ and $\langle \overline{\mathbf{A}} \rangle$ were denoted as the signal subspace in the beam space and $\langle \overline{\mathbf{E}}_n \rangle$ was denoted as the noise subspace in the beam space where $\overline{\mathbf{E}}_s = [\mathbf{v}_1, \cdots, \mathbf{v}_D]$ and $\overline{\mathbf{E}}_n = [\mathbf{v}_{D+1}, \cdots, \mathbf{v}_{3D}]$.

Next, we established OPO on the beam space for projecting the desired source signal subspace, separating the desired source signal from signal sources in the presence of mutual coupling environment. We extracted the desired source signal covariance from the source signal covariance matrix, thereby developing the spectrum algorithm used for source signal DOA estimations. To ensure the algorithm was valid for general applications, we chose the i the source signal as the desired source signal to be estimated. (12) was rewritten as follows:

$$\begin{aligned}
\mathbf{y}(t) &= \overline{\mathbf{a}}(\theta_i) s_i(t) + \sum_{\substack{j=1 \\ j \neq i}}^{D} \overline{\mathbf{a}}(\theta_j) s_j(t) + \overline{\mathbf{n}}(t) \\
&= \overline{\mathbf{a}}(\theta_i) s_i(t) + \mathbf{B}(\theta_i)\mathbf{b}(t) + \overline{\mathbf{n}}(t).
\end{aligned} \tag{16}$$

Here, $\mathbf{B}(\theta_i)$ is the $3D \times (D-1)$ dimensional matrix of $\overline{\mathbf{A}}$ minus $\overline{\mathbf{a}}(\theta_i)$ and $\mathbf{b}(t)$ is the $(D-1) \times 1$ dimensional column matrix of s_i minus $\mathbf{s}(t)$. Because the signal subspace $\langle \overline{\mathbf{E}}_s \rangle$ and noise subspace $\langle \overline{\mathbf{E}}_n \rangle$ were orthogonal, then $\langle \overline{\mathbf{E}}_s \rangle \oplus \langle \overline{\mathbf{E}}_n \rangle = \square^{3D \times 3D}$, where $\oplus$ denoted the direct sum operation of vector subspaces. Let $\alpha_i = E\{s_i s_i^H\}$, and the diagonal element $\mathbf{S}_i$ be the $(D-1) \times (D-1)$ diagonal matrix of $\alpha_l = E\{s_l s_l^H\}$, where $l \neq i$. We obtained the equivalence relation for the signal covariance matrix $\overline{\mathbf{R}}_s$

$$\overline{\mathbf{R}}_s = \begin{cases} \overline{\mathbf{R}}_y - \overline{\mathbf{E}}_n \overline{\mathbf{\Lambda}}_n^2 \overline{\mathbf{E}}_n^H = \overline{\mathbf{A}}\mathbf{S}\overline{\mathbf{A}}^H \\ \overline{\mathbf{a}}(\theta_i)\alpha_i \overline{\mathbf{a}}^H(\theta_i) + \mathbf{B}(\theta_i)\mathbf{S}_i \mathbf{B}^H(\theta_i) \\ \overline{\mathbf{E}}_s \overline{\mathbf{\Lambda}}_s \overline{\mathbf{E}}_s^H. \end{cases} \tag{17}$$

The OPO $\mathbf{O}_{\overline{\mathbf{a}}(\theta_i)|\mathbf{B}(\theta_i)}$ [15–18] was defined as follows:

$$\mathbf{O}_{\overline{\mathbf{a}}(\theta_i)|\mathbf{B}(\theta_i)} = \overline{\mathbf{a}}(\theta_i)(\overline{\mathbf{a}}^H(\theta_i)\mathbf{P}_{\mathbf{B}(\theta_i)}^{\perp}\overline{\mathbf{a}}(\theta_i))^{-1}\overline{\mathbf{a}}(\theta_i)^H \mathbf{P}_{\mathbf{B}(\theta_i)}^{\perp}. \tag{18}$$

Here, $\mathbf{P}_{\mathbf{B}(\theta_i)}^{\perp}$ was the VPO of the range space perpendicular to $\langle \mathbf{B}(\theta_i) \rangle$. According to (18), the range space of $\mathbf{O}_{\overline{\mathbf{a}}(\theta_i)|\mathbf{B}(\theta_i)}$ is $\langle \overline{\mathbf{a}}(\theta_i) \rangle$ and the null space contained $\langle \mathbf{B}(\theta_i) \rangle$. Thus,

$$\mathbf{O}_{\overline{\mathbf{a}}(\theta_i)|\mathbf{B}(\theta_i)} \overline{\mathbf{a}}(\theta_i) = \overline{\mathbf{a}}(\theta_i), \quad \mathbf{O}_{\overline{\mathbf{a}}(\theta_i)|\mathbf{B}(\theta_i)} \mathbf{B}(\theta_i) = 0. \tag{19}$$

$\mathbf{O}_{\overline{\mathbf{a}}(\theta_i)|\mathbf{B}(\theta_i)}$ could be used to remove $\mathbf{B}(\theta_i)$, where $\overline{\mathbf{a}}(\theta_i)$ remained unaffected. This allowed us to separate the desired source signal to be estimated from the other signal sources. The OPO $\mathbf{O}_{\overline{\mathbf{a}}(\theta_i)|\mathbf{B}(\theta_i)}$ differed

from the VPO in (9) and could only be used to remove the subspace perpendicular to the projected space.

To extract the desired signal source variance $E\{(\mathbf{a}(\theta_i)s_i)(\mathbf{a}(\theta_i)s_i)^H\}$ from the signal source covariance matrix, we developed the desired source signal DOA spectrum estimation algorithm. To obtain an accurate estimate $(\overline{\mathbf{a}}(\theta_i)\hat{s}_i)$ of $\overline{\mathbf{a}}(\theta_i)s_i$, we performed an oblique projection on $\langle\overline{\mathbf{a}}(\theta_i)\rangle$ using $\mathbf{y}(t)$, making

$$
\begin{aligned}
\overline{\mathbf{a}}(\theta_i)\hat{s}_i &= \mathbf{O}_{\overline{\mathbf{a}}(\theta_i)|\mathbf{B}(\theta_i)}\mathbf{y}(t) \\
&= \overline{\mathbf{a}}(\theta_i)(\overline{\mathbf{a}}^H(\theta_i)\mathbf{P}_{\mathbf{B}(\theta_i)}^{\perp}\overline{\mathbf{a}}(\theta_i))^{-1}\overline{\mathbf{a}}(\theta_i)^H\mathbf{P}_{\mathbf{B}(\theta_i)}^{\perp}\mathbf{y}(t).
\end{aligned}
\tag{20}
$$

The covariance $E\{(\overline{\mathbf{a}}(\theta_i)s_i)(\overline{\mathbf{a}}(\theta_i)s_i)^H\}$ of signal source was derived from the $\overline{\mathbf{a}}(\theta_i)\hat{s}_i$ second-order statistics $E\{(\overline{\mathbf{a}}(\theta_i)s_i)(\overline{\mathbf{a}}(\theta_i)s_i)^H\}$ using (19) and (20),

$$
\begin{aligned}
E\{\overline{\mathbf{a}}(\theta_i)\hat{s}_i\hat{s}_i^H\overline{\mathbf{a}}(\theta_i)^H\} &= \mathbf{O}_{\overline{\mathbf{a}}(\theta_i)|\mathbf{B}(\theta_i)}E\{\mathbf{y}(t)\mathbf{y}(t)^H\}\mathbf{O}^H_{\overline{\mathbf{a}}(\theta_i)|\mathbf{B}(\theta_i)} \\
&= \mathbf{O}_{\overline{\mathbf{a}}(\theta_i)|\mathbf{B}(\theta_i)}\overline{\mathbf{R}}_y\mathbf{O}^H_{\overline{\mathbf{a}}(\theta_i)|\mathbf{B}(\theta_i)} \\
&= \overline{\mathbf{a}}(\theta_i)\alpha_i\mathbf{a}^H(\theta_i) + \mathbf{O}_{\overline{\mathbf{a}}(\theta_i)|\mathbf{B}(\theta_i)}\overline{\mathbf{E}}_n\overline{\mathbf{\Lambda}}_n^2\overline{\mathbf{E}}_n^H\mathbf{O}^H_{\overline{\mathbf{a}}(\theta_i)|\mathbf{B}(\theta_i)}.
\end{aligned}
\tag{21}
$$

Using (17) and (21), we derived (22) and (23):

$$
\mathbf{O}_{\overline{\mathbf{a}}(\theta_i)|\mathbf{B}(\theta_i)}\overline{\mathbf{R}}_s\mathbf{O}^H_{\overline{\mathbf{a}}(\theta_i)\mathbf{B}(\theta_i)} = \overline{\mathbf{a}}(\theta_i)\alpha_i\overline{\mathbf{a}}^H(\theta_i)
\tag{22}
$$

$$
\mathbf{O}_{\mathbf{B}(\theta_i)|\overline{\mathbf{a}}(\theta_i)}\overline{\mathbf{R}}_s\mathbf{O}^H_{\mathbf{B}(\theta_i)|\overline{\mathbf{a}}(\theta_i)} = \mathbf{B}(\theta_i)\mathbf{S}_i\mathbf{B}^H(\theta_i)
\tag{23}
$$

Using (22) and (23), (24) was obtained:

$$
\begin{aligned}
\mathbf{O}_{\overline{\mathbf{a}}(\theta_i)|\mathbf{B}(\theta_i)}\overline{\mathbf{R}}_s\mathbf{O}^H_{\overline{\mathbf{a}}(\theta_i)|\mathbf{B}(\theta_i)} &+ \mathbf{O}_{\mathbf{B}(\theta_i)|\overline{\mathbf{a}}(\theta_i)}\overline{\mathbf{R}}_s\mathbf{O}^H_{\mathbf{B}(\theta_i)|\overline{\mathbf{a}}(\theta_i)} \\
&= \overline{\mathbf{a}}(\theta_i)\alpha_i\overline{\mathbf{a}}^H(\theta_i) + \mathbf{B}(\theta_i)\mathbf{S}_i\mathbf{B}^H(\theta_i) \\
&= \overline{\mathbf{R}}_s.
\end{aligned}
\tag{24}
$$

Based on (22), we used the OPO $\mathbf{O}_{\overline{\mathbf{a}}(\theta_i)|\mathbf{B}(\theta_i)}$ to extract the desired signal source covariance from $\overline{\mathbf{R}}_s$ .To obtain the desired signal source covariance using (22), $\overline{\mathbf{R}}_s$ and $\mathbf{O}_{\overline{\mathbf{a}}(\theta_i)|\mathbf{B}(\theta_i)}$ must be determined first.The following lemmas show that the pseudo-inverse matrix of $\overline{\mathbf{R}}_s$ ($\overline{\mathbf{R}}_s^+$) could be obtained from the received limited signal samples, which could be used to estimate $\overline{\mathbf{R}}_s$ and produce $\mathbf{O}_{\overline{\mathbf{a}}(\theta_i)|\mathbf{B}(\theta_i)}$ [15–18].

Lemma 3.1:The equation for the OPO $\mathbf{O}_{\overline{\mathbf{a}}(\theta_i)|\mathbf{B}(\theta_i)}$ is as follows:

$$
\mathbf{O}_{\overline{\mathbf{a}}(\theta_i)|\mathbf{B}(\theta_i)} = \overline{\mathbf{a}}(\theta_i)(\overline{\mathbf{a}}^H(\theta_i)\overline{\mathbf{R}}_s^+\overline{\mathbf{a}}(\theta_i))^{-1}\overline{\mathbf{a}}(\theta_i)^H\overline{\mathbf{R}}_s^+
\tag{25}
$$

and

$$
\begin{aligned}
\mathbf{O}_{\overline{\mathbf{a}}(\theta_i)|\mathbf{B}(\theta_i)}\overline{\mathbf{R}}_s\mathbf{O}^H_{\overline{\mathbf{a}}(\theta_i)|\mathbf{B}(\theta_i)} &= \overline{\mathbf{a}}(\theta_i)\alpha_i\overline{\mathbf{a}}(\theta_i)^H \\
&= \overline{\mathbf{a}}(\theta_i)(\overline{\mathbf{a}}^H(\theta_i)\overline{\mathbf{R}}_s^+\overline{\mathbf{a}}(\theta_i))^{-1}\overline{\mathbf{a}}(\theta_i)^H
\end{aligned}
\tag{26}
$$

where $(\overline{\mathbf{a}}^H(\theta_i)\overline{\mathbf{R}}_s^+\overline{\mathbf{a}}(\theta_i))^{-1} = \alpha_i$. Here, $\overline{\mathbf{R}}_s^+ = (\overline{\mathbf{A}}\mathbf{S}\overline{\mathbf{A}}^H)^+ = \overline{\mathbf{E}}_s\overline{\mathbf{\Lambda}}_s^{-2}\overline{\mathbf{E}}_s^H$ was thepseudo-inverse matrixof $\overline{\mathbf{R}}_s$.

Proof: please refer to Appendix I

From Lemma 3.1, we obtained $\overline{\mathbf{R}}_s^+$ from the received limited signal samples to estimate $\overline{\mathbf{R}}_s$. Therefore, $\overline{\mathbf{a}}(\theta_i)$ in (25) was changed to $\overline{\mathbf{a}}(\theta)$ as the scanning steering vector to build a θ_i-related algorithm, where $\theta \in [-90^0, 90^0]$ was scanned to estimate the $\mathbf{O}_{\overline{\mathbf{a}}(\theta_i)|\mathbf{B}(\theta_i)}$. Equation (25)was reordered to produce (27):

$$\mathbf{F}_{\bar{\mathbf{a}}(\theta)} = \bar{\mathbf{a}}(\theta)(\bar{\mathbf{a}}^{H}(\theta)\overline{\mathbf{R}}_{s}^{+}\bar{\mathbf{a}}(\theta))^{-1}\bar{\mathbf{a}}(\theta)^{H}\overline{\mathbf{R}}_{s}^{+} \tag{27}$$

Theorem 3.2[16, 18]:Let

$$\mathbf{G} = \mathbf{F}_{\bar{\mathbf{a}}(\theta)}\overline{\mathbf{R}}_{s}\mathbf{F}_{\bar{\mathbf{a}}(\theta)}^{H} + (\mathbf{P}_{\overline{\mathbf{A}}} - \mathbf{F}_{\bar{\mathbf{a}}(\theta)})\overline{\mathbf{R}}_{s}(\mathbf{P}_{\overline{\mathbf{A}}} - \mathbf{F}_{\bar{\mathbf{a}}(\theta)})^{H}, \tag{28}$$

then

$$\text{Trace}\{\mathbf{G}\} = \text{Trace}\{\overline{\mathbf{R}}_{s}\} + 2\bar{\mathbf{a}}^{H}\mathbf{P}_{\overline{\mathbf{E}}_{n}}(\theta)\bar{\mathbf{a}}(\theta)/(\bar{\mathbf{a}}(\theta)^{H}\overline{\mathbf{R}}_{s}^{+}\bar{\mathbf{a}}(\theta)) \geq \text{Trace}\{\overline{\mathbf{R}}_{s}\}$$

$$= \text{Trace}\{\overline{\mathbf{R}}_{s}\}, \text{ when } \bar{\mathbf{a}}(\theta) = \bar{\mathbf{a}}(\theta_{i}) \tag{29}$$

where $\mathbf{P}_{\overline{\mathbf{A}}}$ was the VPO with $\langle\overline{\mathbf{A}}\rangle$ as the range space.

Proof: please refer to Appendix II

According to (29), when the scanning angle θ was set at $[-90^{0}, 90^{0}]$ and $\bar{\mathbf{a}}^{H}\mathbf{P}_{\overline{\mathbf{E}}_{n}}(\theta)\bar{\mathbf{a}}(\theta)/(\bar{\mathbf{a}}(\theta)^{H}\overline{\mathbf{R}}_{s}^{+}\bar{\mathbf{a}}(\theta))$ equaled zero, we obtained the spatial incidence angle-of-arrival of source signal θ_{i} in a similar way to building a peak in the power spectrum in the beam space to estimate the source signal DOAs.

$$f(\theta) = \max_{\theta} \frac{\bar{\mathbf{a}}(\theta)^{H}\overline{\mathbf{R}}_{s}^{+}\bar{\mathbf{a}}(\theta)}{\left|\bar{\mathbf{a}}^{H}(\theta)\mathbf{P}_{\overline{\mathbf{E}}_{n}}\bar{\mathbf{a}}(\theta)\right|} = \max_{\theta} \frac{\mathbf{a}(\theta)^{H}\mathbf{W}\overline{\mathbf{R}}_{s}^{+}\mathbf{W}^{H}\mathbf{a}(\theta)}{\left|\mathbf{a}(\theta)^{H}\mathbf{W}\overline{\mathbf{E}}_{n}\overline{\mathbf{E}}_{n}^{H}\mathbf{W}^{H}\mathbf{a}(\theta)\right|} \tag{30}$$

We provide the following flowchart to show the procedures of our two-stage algorithm, which is listed below:
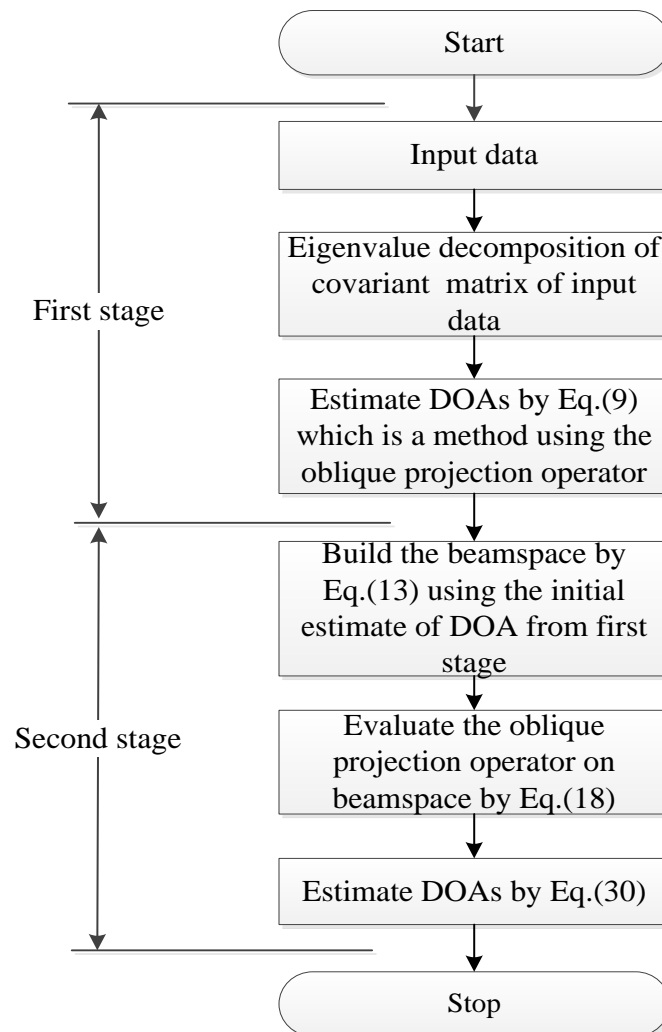

Fig. 1. Flowchart of proposed method

Design Example

In this section, we used computer simulations to demon strate the proposed method's DOA estimation performance for uniform linear arrays.An M number of array sensor elements were found on the uniform linear arrays and the distance between each element was half that of the wavelength. The signal-to-noise ratio (SNR) was the ratio between the signal power and the noise variance of each sensor element.The number of signal sources was known and the zero-mean spatially white Gaussian process was used when performing these simulations.

During the first simulation, threeuncorrelated signal sources entered the system at $\theta_1 = 0^o$, $\theta_2 = 8^o$ and $\theta_3 = 42^o$. The SNR of all the signal sources was 15 dB and the number M of sensor elements was 10 and the mutual coefficients between the sensors are $c_1 = 0.37 + 0.42j$ and $c_2 = 0.09 - 0.21j$. Fig. 2shows the $f(\theta)$ spectrum. The peak of the spectrum demonstrates the angle-of-arrival of the source signal, and DOA estimations still yieldeda high resolution in highly correlated source signal environments.
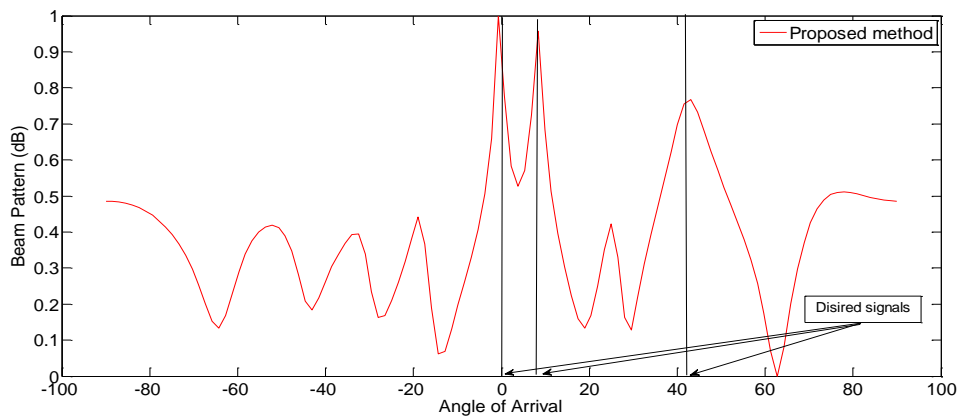

Fig. 2. Normalized spectrum of the proposed method

We used the root mean square error (RMSE) as the performance indicator of the estimation method, where the RMSE of the DOA is as follows

$$RMSE = \sqrt{\sum_{r=1}^{F} \sum_{i=1}^{D} (\theta_i(r) - \theta_i(r))^2 / (FD)} \qquad (31)$$

$\theta_i(r)$ was the estimate of $\theta_i(r)$ during the $r$thMonte Carlo test. We used the RMSE to compare the DOA estimation performance between MUSIC, and our proposed method. All simulations listed below were obtained using1000 Monte Carlo tests.

For the second simulation, we investigated the performance when the SNR ranged from 0 dB to 20 dB; and the number of snapshots was 1000. By projecting the received signal subspace on the beam space to enhance the source signal characteristics, our method can compensate the mutual coupling between sensors and the estimation bias. Fig. 3 shows that our method outperformed the MUSIC methods. The simulations indicated that in a low SNR environment, our proposed method still demonstrated improved performance in such an environment.
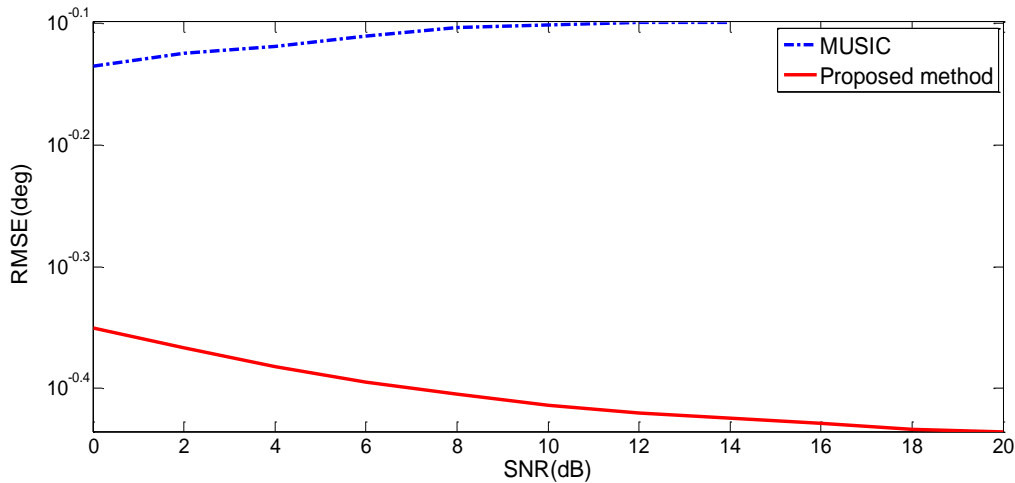
Fig. 3. RMSE of DOA estimations for varying SNRs

Conclusion

In this paper, we introduced a high-resolution estimation method, using the OPO to separate signal sources from the source signal subspace and adopting the beam space to reduce estimation bias of MUSIC in the presence of the mutual coupling environment. Computer simulations results revealed that using oblique projection operator to project appropriate subspace can compensate the mutual coupling error sand that our proposed method yielded superior resolution in the DOA estimation results for signal sources of uniform linear array (ULA) in the presence of mutual coupling.

Appendix

We referred to [15–18] and proposed Lemma 3.1 andTheorem3.2. According to Lemmas 5.3h and 5.9 [23], the pseudo-inverse matrix of $\overline{\mathbf{R}}_s$ in (25) was as follows:

$$\overline{\mathbf{R}}_s^+ = (\overline{\mathbf{A}}\mathbf{S}\overline{\mathbf{A}}^H)^+ = (\overline{\mathbf{A}}^H)^+ \mathbf{S}^{-1}\overline{\mathbf{A}}^+ \tag{32}$$

where $\overline{\mathbf{A}}^+ = (\overline{\mathbf{A}}^H\overline{\mathbf{A}})^{-1}\overline{\mathbf{A}}^H$. Because $\overline{\mathbf{A}} = [\overline{\mathbf{a}}(\theta_i), \mathbf{B}(\theta_i)]$, we obtained the following results using [16,18]:

$$\mathbf{A}^+ = \begin{bmatrix} (\overline{\mathbf{a}}^H(\theta_i)\mathbf{P}_{\mathbf{B}(\theta_i)}^\perp\mathbf{a}(\theta_i))^{-1}\overline{\mathbf{a}}^H(\theta_i)\mathbf{P}_{\mathbf{B}(\theta_i)}^\perp \\ (\mathbf{B}(\theta_i)\mathbf{P}_{\overline{\mathbf{a}}(\theta_i)}^\perp\mathbf{B}(\theta_i))^{-1}\mathbf{B}(\theta_i)\mathbf{P}_{\overline{\mathbf{a}}(\theta_i)}^\perp \end{bmatrix} \tag{33}$$

Based on the definitions of the pseudo-inverse matrix and vertical projection, we derived the following basic characteristics:

$$\overline{\mathbf{R}}_s^+\overline{\mathbf{R}}_s\overline{\mathbf{R}}_s^+ = \overline{\mathbf{R}}_s^+ \tag{34}$$

$$\mathbf{P}_{\overline{\mathbf{A}}}\overline{\mathbf{R}}_s = \overline{\mathbf{R}}_s\mathbf{P}_{\overline{\mathbf{A}}} = \overline{\mathbf{R}}_s \tag{35}$$

Proof of Lemma 3.1

We used (32) and (33) to derive $\overline{\mathbf{a}}^H(\theta_i)\overline{\mathbf{R}}_s^+$, and obtained the following equation:

$$\bar{\mathbf{a}}^{-H}(\theta_i)\overline{\mathbf{R}}_s^+ = \bar{\mathbf{a}}^{-H}(\theta_i)(\overline{\mathbf{A}}\mathbf{S}\overline{\mathbf{A}}^H)^+$$

$$= \bar{\mathbf{a}}^{-H}(\theta_i)(\overline{\mathbf{A}}^H)^+\mathbf{S}^{-1}\overline{\mathbf{A}}^+$$

$$= (\overline{\mathbf{A}}^+\bar{\mathbf{a}}(\theta_i))^H\mathbf{S}^{-1}\overline{\mathbf{A}}^+$$

$$= (\begin{bmatrix} (\bar{\mathbf{a}}^{-H}(\theta_i)\mathbf{P}_{\mathbf{B}(\theta_i)}^{\perp}\bar{\mathbf{a}}(\theta_i))^{-1}\bar{\mathbf{a}}^{-H}(\theta_i)\mathbf{P}_{\mathbf{B}(\theta_i)}^{\perp} \\ (\mathbf{B}(\theta_i)\mathbf{P}_{\bar{\mathbf{a}}(\theta_i)}^{\perp}\mathbf{B}(\theta_i))^{-1}\mathbf{B}(\theta_i)\mathbf{P}_{\bar{\mathbf{a}}(\theta_i)}^{\perp} \end{bmatrix}\bar{\mathbf{a}}(\theta_i))^H\mathbf{S}^{-1}\overline{\mathbf{A}}^+ \quad (36)$$

$$= (\frac{1}{\alpha_i},0,\cdots,0)\overline{\mathbf{A}}^+$$

$$= \frac{1}{\alpha_i}(\bar{\mathbf{a}}^{-H}(\theta_i)\mathbf{P}_{\mathbf{B}(\theta_i)}^{\perp}\bar{\mathbf{a}}(\theta_i))^{-1}\bar{\mathbf{a}}^{-H}(\theta_i)\mathbf{P}_{\mathbf{B}(\theta_i)}^{\perp}$$

We derived (37) from (36):

$$\bar{\mathbf{a}}^{-H}(\theta_i)\overline{\mathbf{R}}_s^+\bar{\mathbf{a}}(\theta_i) = \frac{1}{\alpha_i}(\bar{\mathbf{a}}^{-H}(\theta_i)\mathbf{P}_{\mathbf{B}(\theta_i)}^{\perp}\bar{\mathbf{a}}(\theta_i))^{-1}(\bar{\mathbf{a}}^{-H}(\theta_i)\mathbf{P}_{\mathbf{B}(\theta_i)}^{\perp}\bar{\mathbf{a}}(\theta_i))$$

$$= \frac{1}{\alpha_i} \quad (37)$$

By using (32), (33), and (37), we obtained

$$\bar{\mathbf{a}}(\theta_i)(\bar{\mathbf{a}}^{-H}(\theta_i)\overline{\mathbf{R}}_s^+\bar{\mathbf{a}}(\theta_i))^{-1}\bar{\mathbf{a}}(\theta_i)^H\mathbf{R}_{ss}^+$$

$$= \bar{\mathbf{a}}(\theta_i)\alpha_i\bar{\mathbf{a}}^{-H}(\theta_i)(\overline{\mathbf{A}}^H)^+\mathbf{S}^{-1}\overline{\mathbf{A}}^+$$

$$= \bar{\mathbf{a}}(\theta_i)\alpha_i(\overline{\mathbf{A}}^+\bar{\mathbf{a}}(\theta_i))^H\mathbf{S}^{-1}\overline{\mathbf{A}}^+$$

$$= \bar{\mathbf{a}}(\theta_i)\alpha_i(\begin{bmatrix} (\bar{\mathbf{a}}^{-H}(\theta_i)\mathbf{P}_{\mathbf{B}(\theta_i)}^{\perp}\bar{\mathbf{a}}(\theta_i))^{-1}\bar{\mathbf{a}}^{-H}(\theta_i)\mathbf{P}_{\mathbf{B}(\theta_i)}^{\perp} \\ (\mathbf{B}(\theta_i)\mathbf{P}_{\bar{\mathbf{a}}(\theta_i)}^{\perp}\mathbf{B}(\theta_i))^{-1}\mathbf{B}(\theta_i)\mathbf{P}_{\bar{\mathbf{a}}(\theta_i)}^{\perp} \end{bmatrix}\bar{\mathbf{a}}(\theta_i))^H\mathbf{S}^{-1}\overline{\mathbf{A}}^+ \quad (38)$$

$$= \bar{\mathbf{a}}(\theta_i)\alpha_i(\frac{1}{\alpha_i},0,\cdots,0)\begin{bmatrix} (\bar{\mathbf{a}}^{-H}(\theta_i)\mathbf{P}_{\mathbf{B}(\theta_i)}^{\perp}\bar{\mathbf{a}}(\theta_i))^{-1}\bar{\mathbf{a}}^{-H}(\theta_i)\mathbf{P}_{\mathbf{B}(\theta_i)}^{\perp} \\ (\mathbf{B}(\theta_i)\mathbf{P}_{\bar{\mathbf{a}}(\theta_i)}^{\perp}\mathbf{B}(\theta_i))^{-1}\mathbf{B}(\theta_i)\mathbf{P}_{\bar{\mathbf{a}}(\theta_i)}^{\perp} \end{bmatrix}$$

$$= \bar{\mathbf{a}}(\theta_i)(\bar{\mathbf{a}}^{-H}(\theta_i)\mathbf{P}_{\mathbf{B}(\theta_i)}^{\perp}\bar{\mathbf{a}}(\theta_i))^{-1}\bar{\mathbf{a}}(\theta_i)^H\mathbf{P}_{\mathbf{B}(\theta_i)}^{\perp}$$

According to the definition of $\mathbf{O}_{\bar{\mathbf{a}}(\theta_i)|\mathbf{B}(\theta_i)}$ in (18) and (38), we validated Lemma 3.1.

Proof of Theorem 3.2

For simplicity, we abbreviated $\bar{\mathbf{a}}(\theta)$ as $\bar{\mathbf{a}}$. Using Lemma 3.1 and (34), we obtained

$$\mathbf{F}_{\bar{\mathbf{a}}}\overline{\mathbf{R}}_s\mathbf{F}_{\bar{\mathbf{a}}}^H$$

$$= \bar{\mathbf{a}}(\bar{\mathbf{a}}^{-H}\overline{\mathbf{R}}_s^+\bar{\mathbf{a}})^{-1}\bar{\mathbf{a}}^{-H}\overline{\mathbf{R}}_s^+\overline{\mathbf{R}}_s\overline{\mathbf{R}}_s^+\bar{\mathbf{a}}(\bar{\mathbf{a}}^{-H}\overline{\mathbf{R}}_s^+\bar{\mathbf{a}})^{-1}\bar{\mathbf{a}}^{-H}$$

$$= \bar{\mathbf{a}}(\bar{\mathbf{a}}^{-H}\overline{\mathbf{R}}_s^+\bar{\mathbf{a}})^{-1}\bar{\mathbf{a}}^{-H}\overline{\mathbf{R}}_s^+\bar{\mathbf{a}}(\bar{\mathbf{a}}^{-H}\overline{\mathbf{R}}_s^+\bar{\mathbf{a}})^{-1}\bar{\mathbf{a}}^{-H} \quad (39)$$

$$= \bar{\mathbf{a}}(\bar{\mathbf{a}}^{-H}\overline{\mathbf{R}}_s^+\bar{\mathbf{a}})^{-1}\bar{\mathbf{a}}^{-H}$$

$$= \frac{1}{\bar{\mathbf{a}}^{-H}\overline{\mathbf{R}}_s^+\bar{\mathbf{a}}}\bar{\mathbf{a}}\bar{\mathbf{a}}^{-H}$$

Using (27), (28), (34), (35), (39), and Lemma 3.1, we obtained

$$\mathbf{F_a}\overline{\mathbf{R}}_s\mathbf{F_a}^H + (\mathbf{P_{\overline{A}}} - \mathbf{F_a})\overline{\mathbf{R}}_s(\mathbf{P_{\overline{A}}} - \mathbf{F_a})^H = \frac{2}{\overline{\mathbf{a}}^H\overline{\mathbf{R}}_s^{+}\overline{\mathbf{a}}}\overline{\mathbf{a}}\overline{\mathbf{a}}^H + \overline{\mathbf{R}}_s - \frac{1}{\overline{\mathbf{a}}^H\overline{\mathbf{R}}_s^{+}\overline{\mathbf{a}}}\mathbf{P_{\overline{A}}}\overline{\mathbf{a}}\overline{\mathbf{a}}^H - \frac{1}{\overline{\mathbf{a}}^H\overline{\mathbf{R}}_s^{+}\overline{\mathbf{a}}}\overline{\mathbf{a}}\overline{\mathbf{a}}^H\mathbf{P_{\overline{A}}}$$

$$= \overline{\mathbf{R}}_s + \frac{1}{\overline{\mathbf{a}}^H\overline{\mathbf{R}}_s^{+}\overline{\mathbf{a}}}(\mathbf{I} - \mathbf{P_{\overline{A}}})\overline{\mathbf{a}}\overline{\mathbf{a}}^H + \frac{1}{\overline{\mathbf{a}}^H\overline{\mathbf{R}}_s^{+}\overline{\mathbf{a}}}\overline{\mathbf{a}}\overline{\mathbf{a}}^H(\mathbf{I} - \mathbf{P_{\overline{A}}}) \qquad (40)$$

$$= \overline{\mathbf{R}}_s + \frac{1}{\overline{\mathbf{a}}^H\overline{\mathbf{R}}_s^{+}\overline{\mathbf{a}}}\mathbf{P_{\overline{\mathbf{E}}_n}}\overline{\mathbf{a}}\overline{\mathbf{a}}^H + \frac{1}{\overline{\mathbf{a}}^H\overline{\mathbf{R}}_s^{+}\overline{\mathbf{a}}}.$$

Using (40) and the matrix trace characteristics, we obtained

$$\text{Trace}\{\mathbf{G}\} = \text{Trace}\{\overline{\mathbf{R}}_s + \frac{1}{\overline{\mathbf{a}}^H\overline{\mathbf{R}}_s^{+}\overline{\mathbf{a}}}\mathbf{P_{\overline{\mathbf{E}}_n}}\overline{\mathbf{a}}\overline{\mathbf{a}}^H + \frac{1}{\overline{\mathbf{a}}^H\overline{\mathbf{R}}_s^{+}\overline{\mathbf{a}}}\overline{\mathbf{a}}\overline{\mathbf{a}}^H\mathbf{P_{\overline{\mathbf{E}}_n}}\}$$

$$= \text{Trace}\{\overline{\mathbf{R}}_s\} + \frac{2(\overline{\mathbf{a}}^H\mathbf{P_{\overline{\mathbf{E}}_n}}\overline{\mathbf{a}})}{\overline{\mathbf{a}}^H\overline{\mathbf{R}}_s\overline{\mathbf{a}}} \qquad (41)$$

$$\geq \text{Trace}\{\overline{\mathbf{R}}_s\}$$

When $\mathbf{P_{\overline{\mathbf{E}}_n}}\overline{\mathbf{a}}(\theta_i) = 0$, (29) is valid, thereby confirming the validity of the theorem.

Conflicts of Interest

The authors declare no conflict of interest.

References

1. J. Capon, "High-resolution frequency-wave number spectrum analysis," Proc. IEEE, Vol. 57(1969), pp. 1408-1418.

2. Harry L. Van Trees, Optimum Array Processing, Part IV of Detection, Estimation, and Modulation Theory,John Wiley, New York, 2002.

3. R. O. Schmidt, "Multiple emitter location and signal parameter estimation," IEEE Trans. Antennas and Propagation, Vol. 34(1986), pp. 276–280.

4. R. Roy, and T. Kailath, "ESPRIT-estimation of signal parameters via rotational invariance techniques," IEEE Trans. Acoustics, Speech and Signal Processing, Vol. 37 (1989), pp. 984–995.

5. S. S. Haykin, Communication Systems, John Wiley & Sons, 2000.

6. A. J. Weiss and B. Friedlander, "Mutual coupling effects on phaseonly direction finding," IEEE Trans. Antennas and Propagation, Vol. 40(1992), pp. 535–541.

7. B. C. Ng and C. M. S. See, "Sensor array calibration using a maximum likelihood approach," IEEE Trans. Antennas and Propagation, Vol. 44(1996), pp. 827–835.

8. B. Friedlander and A. J. Weiss, "Direction finding in the presence of mutual coupling," IEEE Trans. Antennas and Propagation,Vol. 39(1991), pp. 273–284.

9. F. Sell one and A. Serra, "A novel online mutual coupling compensation algorithm for uniform and linear arrays," IEEE Trans.Signal Processing,Vol. 55, no. 2(2007), pp. 560–573.

10. T. Svantesson, "Mutual coupling compensation using subspace fitting," inProc. IEEE Sensor Array Multichannel Signal Processing Workshop, Mar. 2000, pp. 494–498.

11. Z. F. Ye, J. S. Dai, X. Xu, and X. P.Wu, "DOA estimation for uniformlinear array with mutual coupling," IEEE Trans. Aerospace and Electronic Systems,Vol. 45, no. 1(2009), pp. 280–288.

12. E. K. L. Hung, "A critical study of a self-calibration direction-finding method for arrays," IEEE Trans.Signal Processing,Vol. 42, no. 2(1994), pp. 471–474.

13. X. Xu, Z. F. Ye, and Y. F. Zhang, "DOA estimation for mixed signals in the presence of mutual

coupling," IEEE Trans.Signal Processing,Vol. 57, no. 9(2009), pp. 3523–3532.

14. B. Liao, Z. G. Zhang, and S. C. Chan, "A subspace-based method for DOA estimation of uniform linear array in the presence of mutual coupling," in Proc. IEEE ISCAS, Paris, France, May 2010, pp. 1879–1882.

15. R. T. Behrens and L. L. Scharf, "Signal processing applications of oblique projection operators," IEEE Trans.Signal Processing,Vol. 42(1994), pp. 1413–1424.

16. M.L. McCloud and L.L. Scharf, "A new subspace identification algorithm for high resolution DOA estimation", IEEE Trans. Antennas and Propagation, Vol. 50, no 10(2002), pp. 1382–1390.

17. X. Xu, Z.F. Ye, and J.H. Peng, "Method of direction of arrival estimation for uncorrelated, partially correlated and coherent sources," IETMicrow Antennas Propagation, Vol. 1, no. 4(2007), pp. 949-954.

18. C. C. Lin, "Using an Oblique Projection Operator for Highly Correlated Signal Direction-of-Arrival Estimation," Applied Mathematics and Information Sciences, Vol. 9 (2015), pp. 2663–2671.

19. S. N. Shahi, M. Emadi, and K. Sadeghi, "High Resolution DOA Estimation in Fully Coherent environments," Progress In Electromagnetics Research C, Vol. 5(2008), pp. 135–148.

20. X.Y. Bu, Z.H. Liu, and K. Yang, "Unbiased DOA estimation for CDMA based on selfinterference cancellation,"Electronics Letter, Vol. 44 (2008), pp. 1163-1165.

21. J.C. Hung and C.C. Lin, "Hybridization of Genetic Algorithm and IBMUSIC applied to DOA estimation under coherent signals", Applied Mathematics & Information Sciences, Vol. 6, no 5S(2012), pp. 495-502.

22. Y. L. Chen and C. C. Lin, "Fuzzy System for DOA Estimation of Coherent Signals", Applied Mechanics and Materials,Vols. 427-429 (2013), pp. 575-581.

23. J.R.Schott,Matrix analysis for statis